Design and Analysis of Strawberry-Picking Industrial Robotic Arm

Adnan Amir
Department of Mechatronics Engineering
SVKM's NMIMS Mukesh Patel School of Technology Management & Engineering
Mumbai, India
adnanamir010@gmail.com

Akshat Verma
Department of Mechanical Engineering
Indian Institute of Technology Bombay
Mumbai, India
akshatneeldev@gmail.com

Abhinav Goswami
Department of Mechanical Engineering
Jorhat Engineering College
Jorhat, India
goswamiabhinav2020@gmail.com

Ashish Kabra
Department of Mechatronics Engineering
Manipal University Jaipur
Jaipur, India
kabraashish789@gmail.com

Shrikar Nakhye
Technical Associate
LearnByResearch
Pune, India
nakhyeshrikar@icloud.com

Sanket Chaudhary
Technical Associate
LearnByResearch
Pune, India
sanketchaudhary31@gmail.com

***Abstract*—Robotic arms have a wide variety of applications in various industries. One of the most important industries where robots can be deployed is agriculture. In this paper, the LearnByResearch(LBR) team has attempted to design a robotic arm to pick and place strawberries in a strawberry plantation. The design is based on the typical dimensions of a strawberry plant. The design and structure of the robot have been justified through kinematic analysis and the Finite Element Method. The robot was simulated in MATLAB to generate the workspace. The research also involves the design of a dedicated control system to control the robot.**

***Index Terms*—Robotics, Manipulators, Mathematical Modelling, Finite Element Analysis**

I. Introduction

The LearnByResearch(LBR) team has designed and simulated a 5 Degree of Freedom(DOF) spatial manipulator which can be used as a harvester robot. The robot has been specifically designed to harvest strawberries. Intensive kinematic analysis and MATLAB simulations were performed to generate the workspace of the robot. The feasibility of the design has been justified through Finite Element Analysis. The research also involves the design of a dedicated control system to control the robot, allowing it to be used to harvest strawberries. The design of the robot is inspired by the design of Puma-560, SCARA and 3-R Serial Manipulator. The robot can pluck strawberries from the branches using a gripper. The robotic manipulator mimics the action of a human arm and the gripper mimics the action of human fingers plucking the fruit.

The robot can reach variable heights which is essential for it to be deployed in non-conventional (hydroponic and aeroponic multi-level) farms. It can also rotate 360 degrees from the same location allowing the arm of the robot to reach different points around it. The robot is mounted over a chassis which is capable of linear motion, thus allowing it to reach different locations on the farm. The chassis can be driven by wheels, tracks etc. The design of the chassis is in itself a vast topic and therefore is out of the scope of this research.

II. Structural Analysis

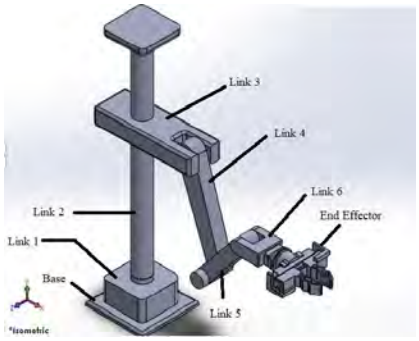

Fig. 1. 3D Model of Manipulator

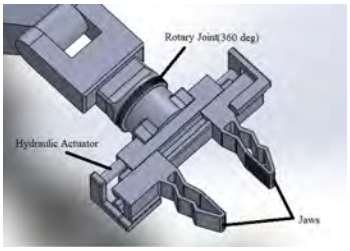

Fig. 2. 3D Model of Gripper

With reference to figure 1, The vertical shaft forming the prismatic joint is connected to the base of the robot by a rotary joint capable of 360° rotation. The prismatic joint allows the

978-1-6654-9291-1/22/$31.00 ©2022 IEEE

end effector to achieve variable height. Following the prismatic joint, there is a revolute joint which forms the shoulder of the robot and another revolute joint forms the elbow of the robot. The wrist of the robot supports the end effector module. With reference to figure 1, the lengths of various links of the robot are, Link 2(vertical column/shaft) is around 100 mm to 500 mm, Link 3(shoulder) is 140 mm, Link 4(elbow) is 220 mm, Link 5(forearm) is 150 mm and Link 6(wrist) is 130 mm.
Figure 2 shows the gripper. The end effector has been designed to mimic the fingers of the human hand plucking strawberries. The end effector does not possess any cutting tool to detach the strawberry from the stalk. Instead, it would grab the strawberry and rotate it by 360° multiple times till it detaches from the stalk. The dimensions of the gripper, like maximum and minimum limits for opening and closing the jaws, are based on the dimensions of typical strawberry fruit. A stereo vision camera can be mounted on the gripper which can analyse the position of the strawberry.
Link 2 constitutes the base of the robot. It plays a very significant role in its static and dynamic stability and vibration damping. The dimensions are mentioned in figure 3

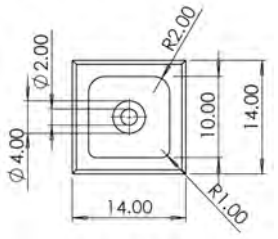

Fig. 3. Dimensions of Base

The degrees of freedom of the manipulator are calculated using the Chebychev-Grubbler-Kutzback criterion, which indicates 5 DOF for this manipulator.

III. Kinematic Analysis of the Serial Manipulator

The kinematic analysis of a robotic manipulator and its given task enables the formulation of fundamental dynamics and control equations [5]. The nonlinear equations developed are utilised to map the joint parameters to the robotic system designed. The Forward Kinematics problem and the Inverse Kinematics problem are performed using MATLAB and analytical processes. This kinematic analysis will allow us to create the robot's workspace and construct an efficient control system.

A. Forward Kinematic Analysis

A serial manipulator comprises multiple links and joints. Forward kinematics analysis is used to determine the total influence of all joint factors. The D-H nomenclature used for specifying serial-link mechanism and geometry is the first step towards robot kinematic analysis. It is crucial to determine the position and orientation of each link in the chain relative to that of the preceding link. The following figure enables us to understand the procedure of assigning

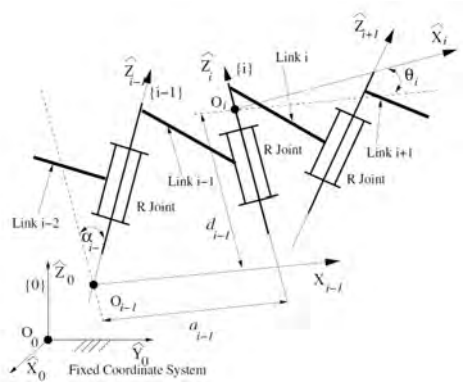

Fig. 4. Assigned coordinate system [6]

the D-H coordinate system to individual joints and links [6], This method was then employed to assign the D-H coordinate system of the 5 DOF manipulator as shown in the following figure(Fig 4).

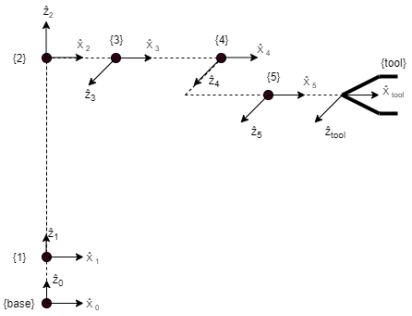

Fig. 5. Kinematic Coordinate System

Using the Kinematic Coordinate System as shown in Fig 4, all the D-H Parameters of the manipulator are listed in Table I. The table consists of the link length(a_{i-1}), offset(d_i), angle of twist(θ_i) and angle between common normal(α_{i-1}).

Serial No.	d_i	θ_i	a_{i-1}	α_{i-1}
1	0	θ_1	0	0
2	d_2	0	0	0
3	0	θ_3	L_2(0.14)	$-\pi/2$
4	$d_4(-0.03)$	θ_4	L_3(0.22)	0
5	0	θ_5	L_4(0.15)	0
6[Tool]	0	0	L_5(0.13)	0

TABLE I
ANALYTICAL DH PARAMETERS
DIMENSIONS WITHIN PARENTHESIS ARE IN MM

The reference frame i can be located relative to reference frame i-1 (fig.4) by executing multiple transformations as shown below and the overall transformation is commonly represented by a 4 × 4 homogeneous transformation as given below,

$$^{0}_{tool}[T] = ^{0}_{1}[T]^{1}_{2}[T]^{2}_{3}[T]^{3}_{4}[T]^{4}_{5}[T]^{5}_{tool}[T]$$

$$
{}^{i-1}_{i}[T] = \begin{bmatrix} c\theta_i & -s\theta_i & 0 & a_{i-1} \\ s\theta_i c\alpha_{i-1} & c\theta_i c\alpha_{i-1} & -s\alpha_{i-1} & -s\alpha_{i-1}d_i \\ s\theta_i s\alpha_{i-1} & c\theta_i s\alpha_{i-1} & c\alpha_{i-1} & c\alpha_{i-1}d_i \\ 0 & 0 & 0 & 1 \end{bmatrix}
$$

On performing a series of transformations of the manipulation, the following transformation equation is obtained,

$$
{}^{0}_{tool}[T] = \begin{bmatrix} \mathrm{N}_x & \mathrm{O}_x & \mathrm{a}_x & \mathrm{P}_x \\ \mathrm{N}_y & \mathrm{O}_y & \mathrm{a}_y & \mathrm{P}_y \\ \mathrm{N}_z & \mathrm{O}_z & \mathrm{a}_z & \mathrm{P}_z \\ 0 & 0 & 0 & 1 \end{bmatrix}
$$

$$
\begin{aligned}
N_x &= \cos\theta_1 \cos(\theta_3 + \theta_4 + \theta_5) \\
N_y &= \sin\theta_1 \cos(\theta_3 + \theta_4 + \theta_5) \\
N_z &= -\sin(\theta_3 + \theta_4 + \theta_5) \\
O_x &= -\cos\theta_1 \sin(\theta_3 + \theta_4 + \theta_5) \\
O_y &= -\sin\theta_1 \sin(\theta_3 + \theta_4 + \theta_5) \\
O_z &= -\cos(\theta_3 + \theta_4 + \theta_5) \\
a_x &= -\sin\theta_1 \\
a_y &= -\cos\theta_1 \\
a_z &= 0
\end{aligned}
$$

$$
P_x = L_2c_1 + L_3c_1c_3 + L_4c_1c_{34} + L_5c_1c_{345} + d_4c_1 \quad (1)
$$

$$
P_y = L_2c_1 + L_3s_1c_3 + L_4s_1c_{34} + L_5s_1c_{345} - d_4c_1 \quad (2)
$$

$$
P_z = d_2 - L_4s_{34} - L_3s_3 - L_5s_{345} \quad (3)
$$

From equations 1,2 and 3, the position of the end effector is described by $P = [(P_xP_yP_z)]^T$, s_{ij}=$sin(\theta_i + \theta_j)$, c_{ij}=$cos(\theta_i + \theta_j)$, s_{ijk}=$sin(\theta_i + \theta_j + \theta_k)$ and c_{ijk}=$cos(\theta_i + \theta_j + \theta_k)$. Here in the DH parameters, d_2 is variable because it is associated with a prismatic joint and the L_5 represents the length of the tool in the end-effector.

The final forward kinematics equations are obtained after replacing all the constant DH parameters with their actual value.

B. Inverse Kinematic Analysis

The pose of the end-effector is related to the joint variables through a non-linear transcendental equation. In order to solve the inverse kinematics problem, these non-linear equations must be solved. The ideal scenario is to obtain a closed-form analytical solution for the location and orientation of the final link. Pure numerical approach can also be employed as shown by Raghavan and Roth [13]. In the inverse kinematics analysis of the manipulator, the primary focus will be on joints 3, 4 and 5 which form the actual manipulator, while assuming joints 1 and 2 to behave like the waist of the robot. This reduces the manipulator to a 3R planar robot and hence simplifies the analysis. The inverse kinematic problem of the manipulator has been solved analytically.

i. Solving θ_1

The θ_1 has been calculated using N_x and N_y which can be obtained from the Forward Kinematics solution in subsection B,

$$
\tan\theta_1 = \frac{N_x}{N_y}
$$

$$
\theta_1 = \tan^{-1}\frac{N_x}{N_y}
$$

ii. Solving θ_4

In figure 6, it can be observed that ΔPQR consists of

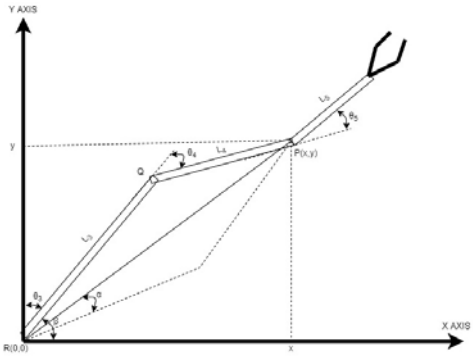

Fig. 6. Graphical Representation of θ_3, θ_4 & θ_5

L_3, L_4 and QR. So, θ_4 can be obtained using the cosine theorem,

$$
X^2 + Y^2 = L_3^2 + L_4^2 - 2L_3L_4\cos(\pi - \theta_4)
$$

$$
\cos\theta_4 = \frac{X^2 + Y^2 - L_3^2 - L_4^2}{2L_3L_4}
$$

Therefore,

$$
\theta_4 = \cos^{-1}\left(\frac{X^2 + Y^2 - L_3^2 - L_4^2}{2L_3L_4}\right)
$$

where $X = P_x - L_5c_1c_{345}$ and $Y = P_y - L_5s_1c_{345}$

iii. Solving θ_3

From the given figure angles α & β can be calculated. Therefore,

$$
\tan\beta = \frac{Y}{X} \qquad \beta = \tan^{-1}\frac{Y}{X}
$$

$$
\cos\alpha = \frac{X^2 + Y^2 + L_3^2 - L_4^2}{2L_3\sqrt{X^2 + Y^2}}
$$

$$
\alpha = \cos^{-1}\left(\frac{X^2 + Y^2 + L_3^2 - L_4^2}{2L_3\sqrt{X^2 + Y^2}}\right)
$$

DH parameter θ_3 is evaluated using the values of angles α and β obtained above as:

$$
\begin{aligned}
\theta_3 &= \alpha + \beta \quad ; \theta_3 > 0 \\
&= \alpha - \beta \quad ; \theta_3 < 0
\end{aligned}
$$

iv. Solving θ_5

Now angle θ_5 can be calculated using the results obtained

from the forward kinematics solution of the robotic manipulator.

$$\tan(\theta_3 + \theta_4 + \theta_5) = \frac{N_z}{O_z}$$

$$\theta_5 = \tan^{-1}\left(\frac{N_z}{O_z}\right) - (\theta_3 + \theta_4)$$

The above-derived equations can be further simplified by substituting all the constant DH parameters like the length of the links(L_3, L_4 & L_5), offsets(d_i) and the twist angle between the joints(α_i), with their real values. Value of θ_1 and θ_5 are obtained from the solution of forward kinematics and other joint angles.

C. Numerical justification of the workspace of the manipulator

The length of links taken can be justified by analysing the angle θ_4,

$$\cos\theta_4 = \frac{X^2 + Y^2 - L_3^2 - L_4^2}{2L_3L_4}$$

$\cos\theta$ exists in the range [-1,1], therefore

$$-1 \leq \frac{X^2 + Y^2 - L_3^2 - L_4^2}{2L_3L_4} \leq 1$$

this implies,

$$(L_3 - L_4)^2 \leq X^2 + Y^2 \leq (L_3 + L_4)^2$$

Here $X = P_x - L_5c_1c_{345}$ and $Y = P_y - L_5s_1c_{345}$
On assuming the height to be momentarily constant and joints 1 and 2 to be the waist of the robot(hence excluding them from the analysis), the workspace obtained is shown in Figure 7.

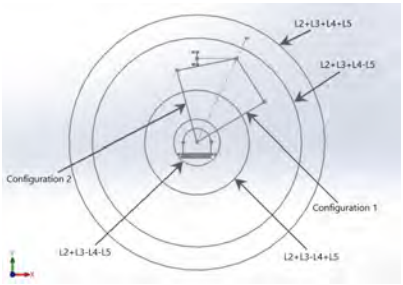

Fig. 7. Projection of the workspace on the $X_0 - Y_0$ plane for $L_3 > L_4 > L_5$

Assuming the height to be momentarily constant, joints 1 and 2 to be the waist of the robot and the links L_2, L_3, L_4 and L_5 to behave like a planar 3R manipulator, the reachable workspace thus obtained is an annular region lying between a circle of radius $L_2 + L_3 + L_4 + L_5$ and $L_2 + L_3 - L_4 - L_5$. The dexterous workspace lies between the other two circles of radii $L_3 + L_4 - L_5$ and $L_3 - L_4 + L_5$ ϕ. Kumar and Waldron [8], [9]

D. Simulation Based Validation

The workspace was simulated using the Monte Carlo method which was chosen based on the results of [2], which was apt for this case. Fig. 8 shows the simulated workspace with the maximum reach of 71.26 cm along the X and Y axes and 99.38 cm along the Z axis.

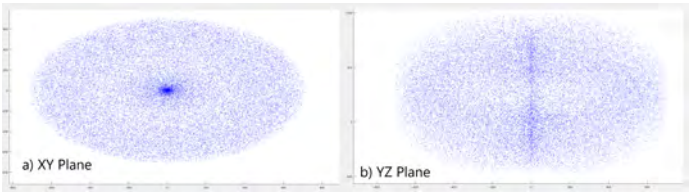

Fig. 8. Monte Carlo Workspace

Reduction as shown in Fig 9, reveals concentric elliptical lines of singularity which finally die off at the 11.2 cm mark. This means that the optimal distance between a strawberry and the robot itself has to be over 11.2 cm, otherwise the strawberry would not fall into the workspace.

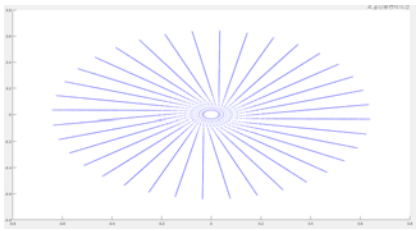

Fig. 9. XY Plane Reduced

The workspaces presented are purely analytical, Practically, the z values would not go below 0, meaning the practical workspace is a hollow semi-ellipsoid.

IV. Modelling and Simulation

The robot is modelled with 5 degrees of freedom. 3 translational along the x,y & z axes and 2 rotational degrees of freedom, namely roll (rotation about the x-axis) and yaw (rotation about the z-axis). However, The yaw is normally locked via programming to keep the end effector parallel to the ground.

Simulation of the manipulator also consists of the aspects listed below which were laid down after careful review and adoption of various techniques used in [11], [3], [14], [10], [7], [1] and [4].
Taking into account the various conditions under which their respective methods of the simulation were applied, a guideline for the simulation was established which involved the following parts:

A DH Parameters
B Inverse Kinematics Solver (Position Controller)
C Control System

A. DH Parameters

The position controller used the Denavit and Hartenberg (DH) convention to make all the mathematical calculations. This convention was preferred over the product of exponentials convention which proves to be complex for robots with a large number of joints, meaning slower calculations.

The verification of the DH parameters was done in RoboAnalyzer, which was also used in [3].

In this paper, two sets of DH parameters were used in the simulation. Table II represents the actual DH parameters of the arm, which were used in the generation of the workspace. Table III contains the other set which will be discussed in subsection B

Joint Number	Joint Type	Joint Angle (θ) (degrees)	Joint Offset (d) (mm)	Link Length (a) (mm)	Twist Angle (α) (degrees)
1	Revolute	Variable	70	0	0
2	Prismatic	0	Variable	227	90
3	Revolute	Variable	0	258	0
4	Revolute	Variable	30	150	0
5	Revolute	Variable	0	80	0

TABLE II
ACTUAL DH PARAMETERS OF THE SIMULATED MANIPULATOR

B. Inverse Kinematics Solver (Position Controller)

The position of the manipulator is controlled through an inverse kinematics script which outputs joint angles based on cartesian coordinate input.

In order to make the calculations less complex and faster, the robot is redesigned as a 4R manipulator. The DH parameters of the redesigned robot are presented in Table III. The controller is programmed to prioritize the translation and rotation of the x and y axes. This is viable only because the prismatic joint affects only the z-axis. So the controller computes joint angles for the x and y position and the height difference is compensated by the prismatic joint.

Joint Number	Joint Type	Joint Angle (θ) (degrees)	Joint Offset (d) (mm)	Link Length (a) (mm)	Twist Angle (α) (degrees)
1	Revolute	0	0	140	90
2	Revolute	Variable	0	220	0
3	Revolute	Variable	300	150	0
4	Revolute	Variable	0	130	0

TABLE III
DH PARAMETERS USED BY POSITION CONTROLLER IN SIMULATION

C. Control System

The control system of the robot was developed in MATLAB Simulink based on the simulations used in [11], [14], [10] and [1]. In the control system, there are 3 basic elements. The Perception Module, The Position Controller and The Robot itself. This can be seen in Fig.10 The perception module may use spatial awareness techniques to generate coordinates for the position controller. Spatial awareness is a vast topic and not in the scope of this research.

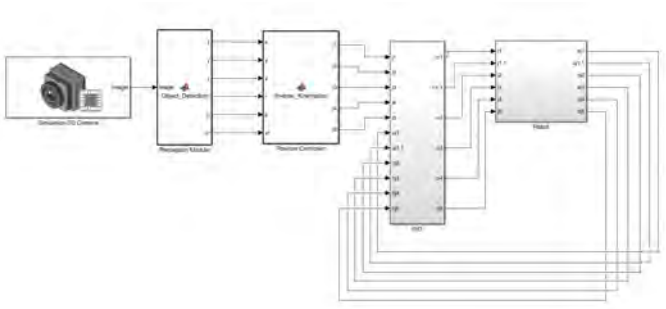

Fig. 10. Simulink Model

The position controller is discussed in detail in subsection B. It is paired with PID control to augment actuation accuracy and eliminate errors due to jerky movement.

V. FINITE ELEMENT MODELING (STRUCTURAL)

The above-explained design for the robotic arm was tested for structural strength and load capacity through finite element analysis of its key components. This analysis included:

- Equivalent Von-Mises Stress distribution and its analysis
- Total Deformation analysis
- Factor of Safety analysis towards yield

The platform used for these was ANSYS Mechanical (2020 R2 version) and static structural studies were set up for the gripper, arm link 1 and arm link 2.

A. Gripper

The material selected for gripper design after manufacturing considerations was Plastic ABS. One finger of the gripper was analyzed under the structural loads calculated. The load capacity of the designed gripper is found to be such that it can easily carry a weight of around 20 kg simultaneously maintaining a safety factor above 2. The obtained FEA results and model well support this claim as illustrated below in figure 11:

B. Arm Link 1 and Arm Link 2

The material for both the arm links was also chosen to be Plastic ABS. The obtained results were as follows, they guaranteed appropriate structural stability along with small deformations of around 1mm in the whole link.

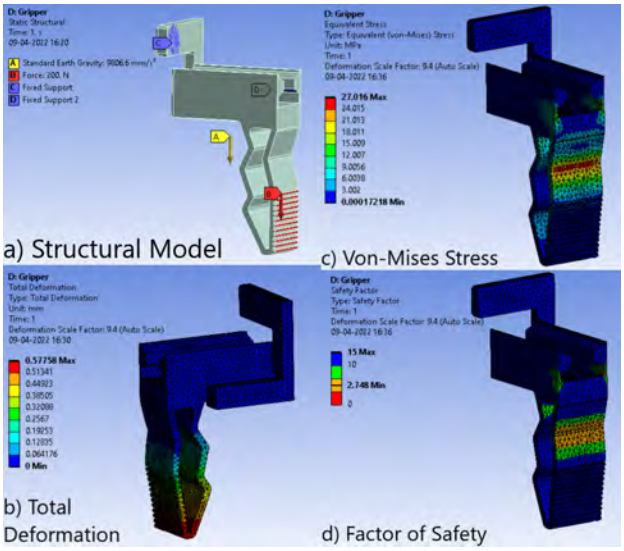

Fig. 11. Gripper

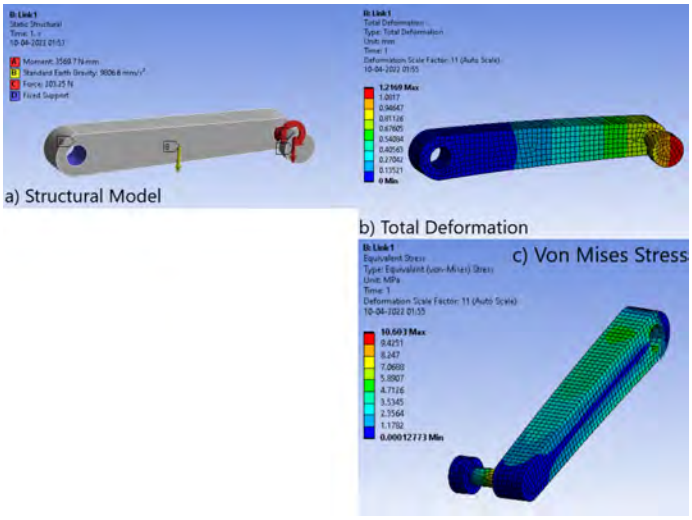

Fig. 12. Arm Link 1

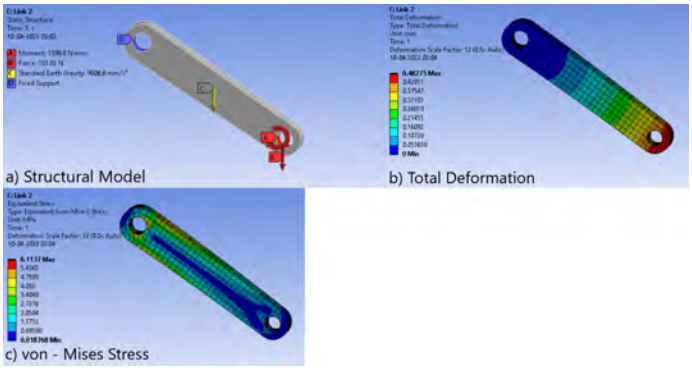

Fig. 13. Arm Link 2

C. Results and Conclusion

The kinematic analysis very well justifies the choice of dimensions for the links to achieve the estimated workspace. The workspace was validated through MATLAB. The results obtained through the FE analysis of the different components of the robotic arm validate its utility in and beyond the expected structural load situations in an efficient manner. The future scope of work lies in implementation. It may involve the optimization of the different arm components for parameters like weight, which can be implemented using the presented simulation results, defining dedicated methods of actuating the links, creating a custom perception algorithm and implementing deep learning as seen in [12].

REFERENCES

[1] Alla N. Barakat, Khaled A. Gouda, and Kenz A. Bozed. Kinematics analysis and simulation of a robotic arm using matlab. Institute of Electrical and Electronics Engineers Inc., 5 2017.

[2] Yi Cao, Ke Lu, Xiujuan Li, and Yi Zang. Accurate numerical methods for computing 2d and 3d robot workspace:. *https://doi.org/10.5772/45686*, 8:76, 1 2011.

[3] Shailendra Singh Chauhan and Avadhesh Kumar Khare. Kinematic analysis of the abb irb 1520 industrial robot using roboanalyzer software. *Evergreen*, 7:510–518, 2020.

[4] M. Taylan Das and L. Canan Dülger. Mathematical modelling, simulation and experimental verification of a scara robot. *Simulation Modelling Practice and Theory*, 13:257–271, 4 2005.

[5] Jacques Denavit. Four-bar coupler-point curves 6-1 the four-bar linkage, 1964.

[6] Ashitava Ghosal. Manipulator kinematics. *HandBook of Manufacturing Engineering and Technology*, pages 1777–1808, 1 2015.

[7] Wong Guan Hao, Yap Yee Leck, and Lim Chot Hun. 6-dof pc-based robotic arm (pc-roboarm) with efficient trajectory planning and speed control. pages 1–7, 7 2011.

[8] A. Kumar and K. J. Waldron. The dexterous workspace. *ASME paper no*, 80-DET-108, 1980.

[9] A Kumar and K J Waldron. The workspaces of a mechanical manipulator. *Journal of Mechanical Design*, 103:665–672, 7 1981.

[10] Kichang Lee, Jiyoung Lee, Bungchul Woo, Jeongwook Lee, Young Jin Lee, and Syungkwon Ra. Modeling and control of a articulated robot arm with embedded joint actuators. *2018 International Conference on Information and Communication Technology Robotics, ICT-ROBOT 2018*, 11 2018.

[11] Dinh Tho Long, To Van Binh, Roan Van Hoa, Le Van Anh, and Nguyen Van Toan. Robotic arm simulation by using matlab and robotics toolbox for industry application. *International Journal of Electronics and Communication Engineering*, 7, 2020.

[12] Xiaohan Ni, Xin He, and Takafumi Matsumaru. Training a robotic arm movement with deep reinforcement learning. In *2021 IEEE International Conference on Robotics and Biomimetics (ROBIO)*, pages 595–600, 2021.

[13] M Raghavan and B Roth. Inverse kinematics of the general 6r manipulator and related linkages. *Journal of Mechanical Design*, 115:502–508, 9 1993.

[14] Jargalbaatar Yura, Mandakh Oyun-Erdene, Bat Erdene Byambasuren, and Donghan Kim. Modeling of violin playing robot arm with matlab/simulink. *Advances in Intelligent Systems and Computing*, 447:249–261, 2017.